CORROSION SCIENCE AND TECHNOLOGY, Vol.22, No.1(2023), pp.30~35 pISSN 1598-6462 / eISSN 2288-6524
[Research Paper] DOI: https://doi.org/10.14773/cst.2023.22.1.30

Mechanical and Structural Behaviors of HfN Thin Films Fabricated by Direct Current and Mid-frequency Magnetron Sputtering

Sung-Yong Chun†

Department of Advanced Materials Science and Engineering, Mokpo National University, Jeonnam 58554, Korea
(Received December 13, 2022; Revised December 26, 2022; Accepted December 26, 2022)

Hafnium nitride (HfN) thin films were fabricated by mid-frequency magnetron sputtering (mfMS) and direct current magnetron sputtering (dcMS) and their mechanical and structural properties were compared. In particular, changes in the HfN film properties were observed by changing the pulse frequency of mfMS between 5 kHz, 15 kHz, and 30 kHz. The crystalline structure, microstructure, 3D morphology, and mechanical properties of the HfN films were compared by x-ray diffraction, field-emission scanning electron microscopy, atomic force microscopy, and nanoindentation tester, respectively. HfN film deposited by mfMS showed a smoother and denser microstructure as the frequency increased, whereas the film deposited by dcMS showed a rough and sloppy microstructure. A single δ-HfN phase was observed in the HfN film made by mfMS with a pulse frequency of 30 kHz, but mixed δ-HfN and $HfN_{0.4}$ phases were observed in the HfN film made by dcMS. The mechanical properties of HfN film made by mfMS were improved compared to film made by dcMS.

Keywords: *Pulse frequency, Direct current, Thin film, Magnetron sputtering, HfN*

1. Introduction

Thin film materials made of transition metal nitride, exhibiting properties of high hardness, high elasticity, and high abrasion resistance, are broadly used as a coating material for tools and components of diverse kinds of machines [1-3]. Among them, the HfN manifests excellent properties of high melting point (3,380 °C), high hardness (16.3 GPa), low resistance (33 μΩ·cm), and chemical inertness etc. by which it became the compound having the lowest enthalpy among single nitrides of transition metals having rock-salt structure (lattice constant = 4.525Å). Owing to such excellent properties, the applications of the material for optical thin films, electrodes in devices in semiconductors, diffusion barriers, and materials for buffer layer are reported as well [4]. Several deposition methods comprising magnetron sputtering, pulse laser deposition, or metal-organic chemical vapor deposition (MOCVD) etc. are reported, and among them, the magnetron sputtering is broadly employed because it allows excellent reproducibility and higher speed of deposition [5-8].

†Corresponding author: sychun@mokpo.ac.kr
Sung-Yong Chun: Professor

However, the dcMS exhibits the disadvantage of low mobility of low-energy atoms on surface of substrates resulting in easy creation of thin film of columnar structure due to lower level of energy of sputtered target particles [9]. Thus, in the present study, the mfMS which is being spotlighted on its capability of controlling parameters of pulse plasma and conventional dcMS was employed for the preparation of HfN film. In particular, the pulse frequency and duty cycle among parameters in the mfMS process as well as effects thereof upon crystal structure and microstructure of coating film were observed. mfMS exploits the power supply of pulse direct current instead of the direct current power supply used for dcMS thereby the generation of arc is fundamentally suppressed due to the presence of time releasing positive (+) voltage. Therefore, it can prevent the generation of defects in specimens to be created by micro-arcs, and has an advantage of rising stability of plasma. Besides, mfMS enables the creation of plasma, having the ion flux embedding higher level of ion energy comparing to dcMS, thereby it is expected to improve mechanical properties or microstructure of thin film [10].

Recently, the fabrication of HfN film by using radio-frequency magnetron sputtering (rfMS) or high-power

impulse magnetron sputtering (HiPIMS) has been reported however the studies, reported the effects of plasma process parameters such as pulse frequency and duty cycle upon mechanical properties of HfN film, are yet to be reported [11-13]. Thus, in this study, the HfN films were prepared by employing dcMS and mfMS comprising three mid-frequency plasma process conditions for the comparison of mechanical properties of HfN films, wherein the effects of plasma process parameters upon 2D microstructures such as crystal structures, surfaces, and cross sections of film, and upon 3D microstructures such as morphologies, were examined.

2. Experimental Methods

HfN thin films were grown on Si (100) substrate by dcMS and mfMS at four different sputtering conditions. Before deposition, the substrate was dried after cleaning in the ultrasonic cleaning apparatus with acetone and ethyl alcohol respectively for 10 minutes. In the experiment conducted in the present study, the HfN thin films were fabricated from the four process conditions comprising one process condition of dcMS and three mid-frequency process conditions of mfMS. The experimental conditions of single chamber and process atmosphere were kept for the comparison of properties of HfN film fabricated under different conditions; the pulse frequency and duty cycle among process conditions of mfMS were varied for the fabrication of HfN film. Further details of the process conditions of fabrication of HfN film are as presented in Table 1. Hf round target with the purity of 99.99% was used as a starting material. Ultrahigh purity N_2 and Ar gases were also used for the process with the ratio of Ar (31 sccm) and N_2 (5 sccm). The distance between target and substrate was about 60 mm. The substrate was rotated at the speed of 10 rpm. The initial vacuum level of chamber was at the level of 4.0×10^{-4} Pa. Preliminary sputtering using Ar gas was carried out to clean the substrate and target before deposition, The Grazing Incidence X-ray Diffraction (HighScopre Plus, Pananalytical) was used to analyze the crystalline structure of the HfN films while the Field Emission SEM (S-3500N, Hitachi) and Atomic Force Microscopy (Dimension Icon, Bruker) were used for the observation of 2D and 3D microstructures and morphologies thereof. Besides, the Nanoindentation Tester (NHT3, Anton Paar) was used for the higher force instrumented indentation testing of thin film. Visual matrices of indentations and continuous multi cycles (CMC) were conducted to measure the mechanical properties as a function of position on the surface and depth in the sample.

3. Results and discussion

3.1 Crystalline structure

Crystalline structure determination of HfN thin films deposited under four different fabrication process conditions of dcMS and mfMS, are presented in Fig. 1. The δ-HfN (111), (220), and (311) surface peaks were observed from all HfN film, whereas the film, fabricated under condition 1, condition 2, and condition 3 of dcMS and mfMS, exhibited the $HfN_{0.4}$ (101) and (103) surface peaks as well as δ-HfN peaks. However, in the HfN film fabricated under condition 4 of mfMS, the coating film of δ-HfN single phase was created without further observations of $HfN_{0.4}$ peaks. That is, the dominant δ-HfN crystal phases and tiny amount of $HfN_{0.4}$ crystal phases were analyzed in the HfN film fabricated under process condition of dcMS and process conditions of mfMS similar to dcMS, whereas in the HfN film fabricated under condition 4 of mfMS of the highest pulse frequency (30 kHz) with the lowest duty cycle (70%), only the δ-HfN single phase was present. From results above, the changes and

Table 1. Conditions for deposition of HfN films using dcMS and mfMS

Conditions	1	2	3	4
Sputtering (type)	dcMS	mfMS	mfMS	mfMS
Sputtering Power (W)	300	300	300	300
Pulse frequency (kHz)	-	5	15	30
Duty cycle (%)	-	95	85	70
Substrate bias voltage (V)	-100	-100	-100	-100

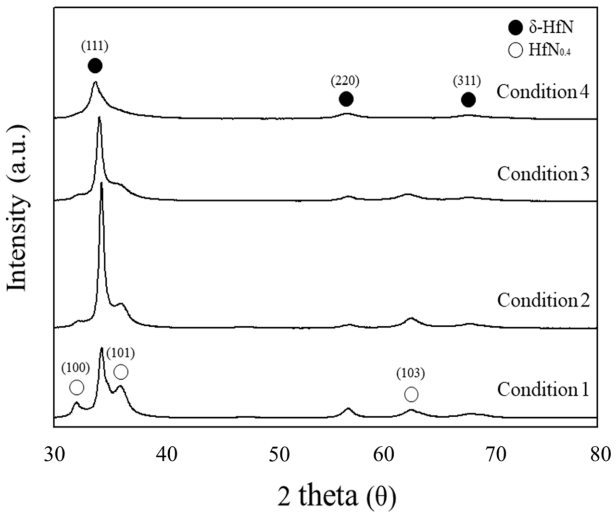

Fig. 1. XRD data of HfN films fabricated by dcMS and mfMS

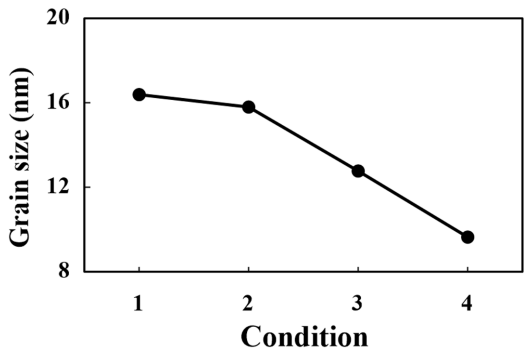

Fig. 2. Average size of crystal grains of HfN films fabricated by dcMS and mfMS

controllability of crystal phases of film according to med-frequency process parameters of mfMS, comparing to those of dcMS, were identified.

3.2 Size of crystallites

Average size of crystallites of film is a critical element determining properties of film applicable to diverse fields. In general, the decrease in size of crystallites of film of high hardness and high abrasion resistance results in the increase of residual stress and hardness by which the adhesive force and anti-abrasion resistance of coating film increases. Therefore, the accurate measurement of the size of crystallites of film is crucial for the optimization of application of coating film. In general, the employment of transmission electron microscope for the measurement of the size of crystallites would require a lot of time and cost for the preparation of specimens and observation. Therefore, the x-ray diffraction analysis appeared as a simplified and improved new approach for the measurement of the size of crystallites in coating film. The size of crystallites was calculated by Debye-Scherrer equation wherein the size of crystallites appeared decreasing in accordance with increasing full width half maximum (FWHM) [15]. Besides, the results, corrected by using the standard sample of bulk HfN, was used for the correction of errors created by the intrinsic instrumental width of the equipment; the resulted formula is as presented below:

$$D = K \cdot \lambda / \beta \cdot \cos\theta$$

Where D is the size of the crystal grains, K is known as the Scherer's constant (K=0.94), λ is the X-ray wavelength (1.54178Å), β is full width at half maximum (FWHM) of the diffraction peak and θ is the Bragg angle. Average sizes of crystallites of the four HfN films, varied according to respective process conditions, are presented in Fig. 2. The results of the average size of crystallites in HfN films show continuous decrease of 16.4 nm (condition 1), 15.8 nm (condition 2), 12.8 nm (condition 3), and 9.6 nm (condition 4) according to the employment of mfMS and process conditions of mid-frequency. That is, HfN film fabricated under condition 1 by employing dcMS rendered the biggest size of crystallite, whereas the smallest size of crystallites of HfN film prepared through condition 4 of mfMS appeared. In our laboratory, we have reported previously the tendency of decreasing size of crystallites in HfN film according to the employment of mfMS using transition metal compounds such as TiN or CrN having crystal structure similar to NaCl [15].

3.3 Microstructure

Microstructures of HfN film, fabricated under four process conditions, were analyzed using Field Emission SEM; the surfaces and cross-sections thereof are as presented in Fig. 3. Above all, the polycrystalline fine crystal grains on the surfaces of HfN films fabricated under condition 1 and condition 2, and microstructures having macro crystal grains of columnar structure developed perpendicular to substrates in the cross sections of HfN thin films, were observed. On the contrary, the

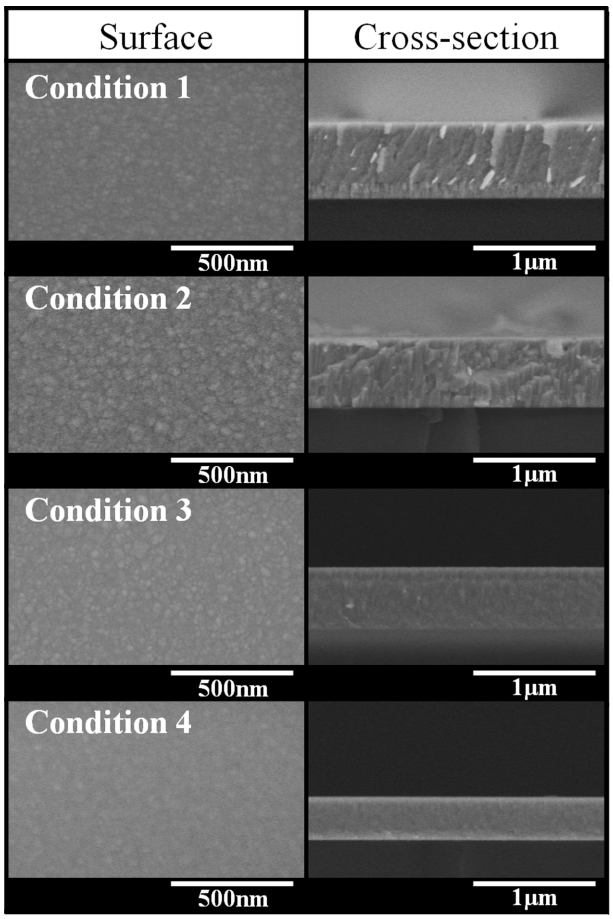

Fig. 3. Surface and cross-section Field Emission SEM images of HfN films fabricated by dcMS and mfMS

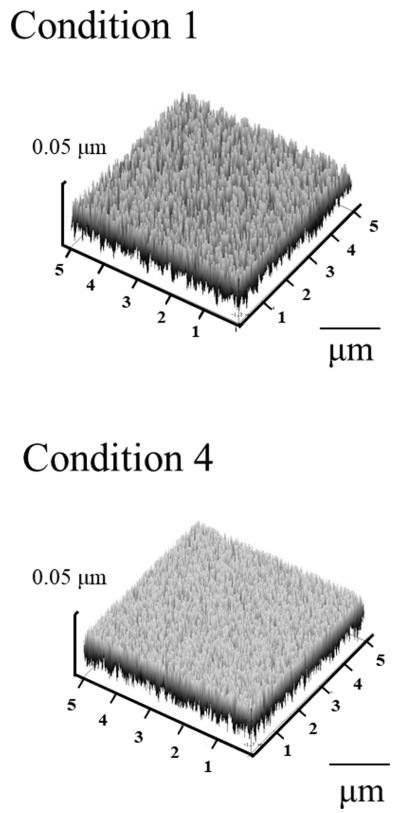

Fig. 4. SPM surface morphologies of HfN films fabricated by dcMS and mfMS

image of reduced contrast of polycrystalline fine crystal grains from the surfaces of HfN thin films prepared under condition 3 and condition 4, and the dense microstructure, wherein the macro crystal grains of columnar structure disappeared from the cross sections of HfN films, were observed. This suggests the plasma process parameters in mfMS acted as crucial factors that determined the microstructure of thin film. The densification of microstructure together with refinement of crystal grains are attributed to the creation of atoms of energy at least maximum 100 times higher than those created in the dsMS [16].

3.4 3D morphology

The 3D morphologies of HfN films prepared by employing dcMS and mfMS were observed through using noncontact SPM analysis, and the results are as presented in Fig. 4. The results of analysis of morphology revealed the smoothness and homogeneousness of the surface of HfN thin film prepared under condition 4 which appeared most excellent than those prepared under condition 1. Actual measurements of surface roughness (Ra) of HfN thin film obtained from condition 1 and condition 4 of both dcMS and mfMS appeared as 10.1 nm and 7.2 nm, respectively. Thus, the most excellent surface roughness reduced by approximately maximum 30% was obtained from the HfN thin film prepared under condition 4 of mfMS. This was attributed to the creation of depositing atoms of higher energies exhibiting higher mobility on the surface of substrate that resulted in excellent surface characteristics approximately 30% to 80% improved with the employment of mfMS comparing to the employment of dcMS [17].

3.5 Nanoindentation hardness

Precise measurement of surface mechanical properties such as hardness and elastic modulus in the level of nanometer scale is difficult to obtain due to the size effect. To remove the size effect of nanoindentation such as increasing hardness with shallower depth of indentation, the measurement of nanoindentation hardness was

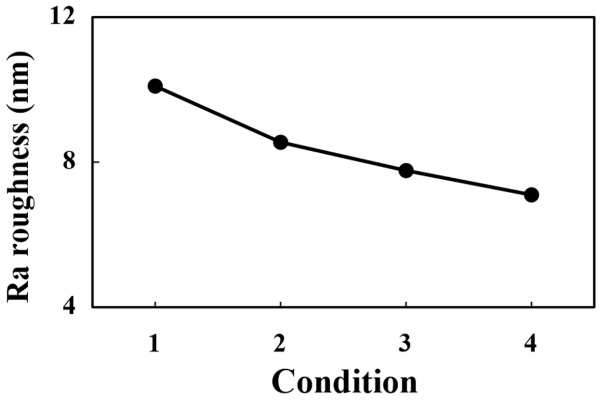

Fig. 5. Ra roughness data of HfN films fabricated by dcMS and mfMS

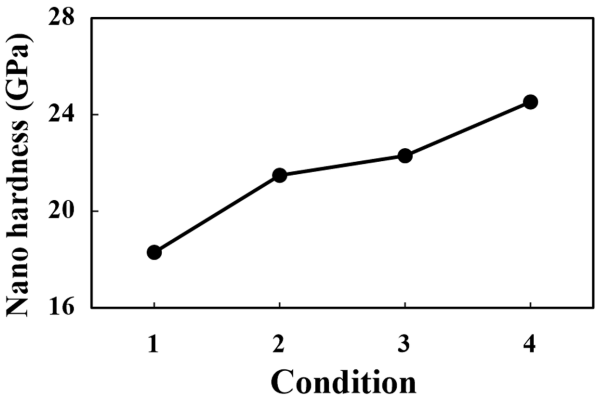

Fig. 6. Nanoindentation hardness of HfN films fabricated by dcMS and mfMS

analyzed at the points of 1/10 of thickness of thin film. Therefore, careful calibration of both instrument and indenter shape in the relevant standards (ISO 14577-4) were taken into account for precise measurement. The results of nanoindentation hardness followed by above standards to HfN films fabricated by dcMS and mfMS are presented in Fig. 5. The figure shows the highest nanoindentation hardness of HfN film deposited under condition 4 of mfMS. Measurement of nanoindentation hardness of thin film prepared under condition 1, condition 2, condition 3, and condition 4 appeared as 18.3 GPa, 21.5 GPa, 22.3 GPa, and 24.5 GPa, respectively showing the sequential increase in accordance with increasing pulse frequency and decreasing duty cycle, wherein the nanoindentation hardness of HfN thin film fabricated under condition 4 of mfMS increased approximately 75% comparing to the lowest nanoindentation hardness of HfN film fabricated by using dcMS.

4. Conclusions

In this study, a total of four different kinds of HfN thin films were fabricated by dcMS and mfMS. The properties of crystalline structure and microstructure of HfN thin films were compared each other. The crystalline structure and microstructure of HfN thin films showed a distinct dependence on the process conditions. The HfN film fabricated under condition 4 rendered δ-HfN single phase solely, whereas the HfN films fabricated under condition 1, condition 2, and condition 3 rendered the weak $HfN_{0.4}$ (100), (101), and (103) surface peaks besides the δ-HfN peak. The polycrystalline fine crystal grains on the surfaces and macro crystal grains of columnar structure developed perpendicular to substrate in the cross section of HfN films fabricated under condition 1 and condition 2 were observed, whereas on the surfaces and cross sections of HfN films fabricated under condition 3 and condition 4, the smooth crystal grains and dense microstructures consisted of fine crystal grains were observed. The excellent crystallographic, microstructural and mechanical properties of HfN film fabricated by mfMS comparing to the HfN films prepared by dcMS were attributed to the creation of depositing atoms of higher energy and higher mobility on the surfaces of substrate.

Acknowledgements

This Research was supported by Research Funds of Mokpo National University in 2022.

References

1. S. Y. Chun, S. J. Kim, Enhancement of the Corrosion Resistance of CrN Film Deposited by Inductively Coupled Plasma Magnetron Sputtering, *Corrosion Science and Technology*, **20**, 112 (2021). Doi: https://doi.org/10.14773/cst.2021.20.3.112
2. S. Y. Chun, S. W. Park, A Comparative Study of CrN Coatings Deposited by DC and Pulsed DC Asymmetric Bipolar Sputtering for a Polymer Electrolyte Membrane Fuel Cell (PEMFC) Metallic Bipolar Plate, *Journal of the Korean Ceramic Society*, **50**, 390 (2013). Doi: https://doi.org/10.4191/kcers.2013.50.6.390
3. S. Y. Chun, J. Y. Hwang, Effects of Duty Cycle and Pulse

Frequency on the Microstructure and Mechanical Properties of TiAlN Coatings, *Journal of the Korean Ceramic Society*, **51**, 447 (2014). Doi: https://doi.org/10.4191/kcers.2014.51.5.447

4. Y. S. Fang, K. A. Chiu, H. Do, L. Chang, Reactive sputtering for highly oriented HfN film growth on Si (100) substrate, *Surface and Coatings Technology*, **377**, 124877 (2019). Doi: https://doi.org/10.3390/coatings10070647
5. R. Armitage, Q. Yang, H. Feick, J. Gebauer, E. R. Weber, Lattice-matched HfN buffer layers for epitaxy of GaN on Si, *Applied Physics Letters*, **81**, 1450 (2002). Doi: https://doi.org/10.1063/1.1501447
6. J. J. Oakes, A comparative evaluation of HfN, Al_2O_3, TiC and TiN coatings on cemented carbide tools, *Thin Solid Films*, **107**, 159 (1983). Doi: https://doi.org/10.1016/0040-6090(83)90018-4
7. X. M. Cai, F. Ye, E.Q. Xie, D.P. Zhang, P. Fan, Field electron emission from HfNxOy thin films deposited by direct current sputtering, *Applied Surface Science*, **254**, 3074 (2008). Doi: https://doi.org/10.1016/j.apsusc.2007.10.058
8. I.E. Fragkos, N. Tansu, Surface plasmon coupling in GaN:Eu light emitters with metal-nitrides, *Scientific Reports*, **8,** 13365 (2018). Doi: https://doi.org/10.1038/s41598-018-31821-8
9. S. Y. Tan, X. H. Zhang, X. J. Wu, F. Fang, J. Q. Jiang, Comparison of chromium nitride coatings deposited by DC and RF magnetron sputtering, *Thin Solid Films*, **519,** 2116 (2011). Doi: https://doi.org/10.1016/j.tsf.2010.10.067
10. R. D. Arnell, P. J. Kelly, J. W. Bradley, Recent developments in pulsed magnetron sputtering, *Surface and Coatings Technology*, **188–189,** 158 (2004). Doi: https://doi.org/10.1016/j.surfcoat.2004.08.010
11. R. Nowak, S. Maruno, Surface deformation and electrical properties of HfN thin films deposited by reactive sputtering, *Materials Science and Engineering: A*, **202**, 226 (1995). Doi: https://doi.org/10.1016/0921-5093(95)09814-3
12. B. H. Hwang, S. Y. Chiou, An XRD study of highly textured HfN films, *Thin Solid Films*, **304**, 286 (1997). Doi: https://doi.org/10.1016/S0040-6090(97)00106-5
13. W. Tillmann, N. F. L. Dias, D. Stangier, M. Tolan, M. Paulus, Structure and mechanical properties of hafnium nitride films deposited by direct current, mid-frequency, and high-power impulse magnetron sputtering, *Thin Solid Films*, **669,** 65 (2019). Doi: https://doi.org/10.1016/j.tsf.2018.10.035
14. B. D. Cullity and S. R. Stock, *Elements of X-Ray Diffraction, 3rd. ed.*, pp. 167 - 171, Prentice-Hall Inc., New York (2001).
15. I. Petrov, P. B. Barna, L. Hultman, J. E. Greene, J. Vac. Microstructural evolution during film growth, *Sci. Tech. A*, **21**, S117 (2003). Doi: https://doi.org/10.1116/1.1601610
16. D. Ö. Thorsteinsson and J. T. Gudmundsson, Growth of HfN thin films by reactive high power impulse magnetron sputtering, *AIP Advances*, **8**, 035124 (2018). Doi: https://doi.org/10.1063/1.5025553
17. J. Lin, I. Dahan, B. Valderrama, and M. V. Manuel, Structure and Properties of Uranium Oxide Thin Films Deposited by Pulsed DC Magnetron Sputtering, *Applied Surface Science*, **301,** 475 (2014). Doi: https://doi.org/10.1016/j.apsusc.2014.02.106